Peak heights[a.u]	Cross-correlation frequency	Autocorrelation frequency
30-40	86	0
40-50	224	0
50-60	308	0
60-70	360	0
70-80	295	0
80-90	102	0
90-100	27	0
* 100-110	4	0
110-120	0	0
** 120-130	0	1
130-140	0	8
140-150	0	15
150-160	0	8
160-170	0	5
170-180	0	0
180-190	0	0
190-200	0	1

* Maximum Cross-correlations
** Minimum Autocorrelation

CThO40 Fig. 3. Experimental study of cross-correlation signal height distribution for all partial characters (38 × 38 = 1444).

introduced in a parallel JTC recognition system. It improved the discrimination tolerance significantly by using six times smaller pixel numbers of 25 × 25 as compared to the previous 64 × 64. The result ensures the throughput acceleration by increasing parallelism while keeping improved discrimination signal quality.

We thank M. Tsuchiya of the University of Tokyo for enlightening discussions.

Japan Women's University, Department of Mathematical and Physical Science, 2-8-1 Mejirodai, Bunkyo-ku, Tokyo-112, Japan

1. J.W. Goodman, *Introduction to Fourier Optics*, 2nd ed. (McGraw-Hill, New York, 1996), Chapt. 8.
2. R. Thapliya *et al.*, Proc. CLEO/Pacific Rim '97 (IEEE/LEOS, 1997), paper FW4, pp. 310–311.
3. R. Thapliya *et al.*, Opt. Rev. **3**, 397–399 (1996).
4. K. Kodate *et al.*, Proc. CLEO/Pacific Rim '97 (IEEE/LEOS 1997), paper FK3, pp. 276–277.
5. K. Kodate *et al.*, Opt. Rev. **3**, 400–402 (1996).

CThO41

Miniature nonlinear optical-loop mirrors with semiconductor optical amplifiers

Jinn-Haw Lee, Hsin-Jiun Chiang, Steffen Gurtler, C.C. Yang, *College of Electrical Engineering, National Taiwan University, 1, Roosevelt Road, Section 4, Taipei, Taiwan, R.O.C.; E-mail: jhlee@crlisaf.ee.ntu.edu.tw*

Nonlinear optical-loop mirrors are important devices for all-optical switching and other applications. Typically, such a device consists of an optical fiber loop connected to a fiber coupler. The required optical nonlinearity may come from the Kerr effect in fiber or gain saturation in an inserted semiconductor optical amplifier. Such a device with 1.5 m fiber loop length has a latency as large as 10 ns. In this paper, we present our experimental results of miniature nonlinear optical-loop mirrors made of GaAs/AlGaAs quantum-well optical amplifiers. The layout of such a device is shown in Fig. 1. The ridge-loading waveguide loop has a 300-μm radius with a 4-μm ridge width. The loop is connected to a multimode interference (MMI) waveguide 500 μm in length and 8 μm ridge width. Then the input and output ports are also 4-μm waveguides with both lengths ~100 μm. For injecting different currents in different areas, we divided the electropad into four disconnected regions, indicated by the injection currents I_1 (input-output region), I_2 (MMI region), I_3 (one quarter of loop), and I_4 (three quarters of loop). I_3 and I_4 are always different to break the symmetry of the two counterpropagating signals in the loop. The device shown in Fig. 1 should lead to a latency of 30 ps.

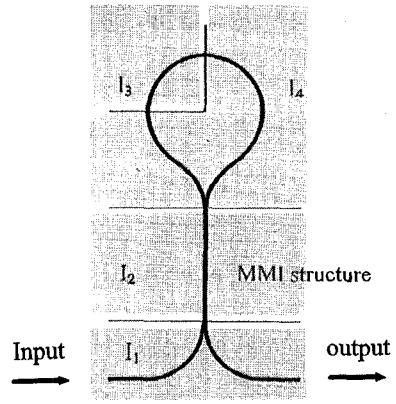

CThO41 Fig. 1. Layout of a miniature nonlinear optical-loop mirror.

The epitaxial structure of the semiconductor optical amplifier consisted of five GaAs wells (6.5 nm in thickness) and four $Al_{0.25}Ga_{0.75}As$ barriers (20 nm in thickness), leading to a photoluminescence peak of ~840 nm. To improve the quality of the curved waveguide in the loop so that the bending loss could be reduced, we used the cryoetching technique to etch the samples. With samples inside a chamber filled with Cl_2 gas (~1 mTorr) and irradiated by a 193-nm excimer laser at a low temperature (~125 K), high-quality etching walls could be obtained. The etching depth was ~1.8 μm, which reached the upper separate confinement layer. Figure 2 shows the top view of a finished device under a microscope.

Figure 3 demonstrates three sets of data showing power-dependent switching. We launched a cw Ti:sapphire laser at 840 nm with various power levels and monitored the output

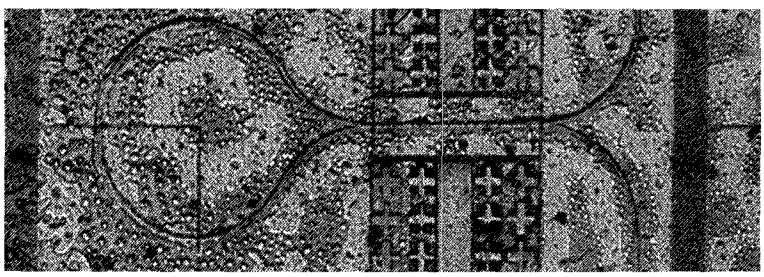

CThO41 Fig. 2. Top view of a finished miniature nonlinear optical-loop mirror.

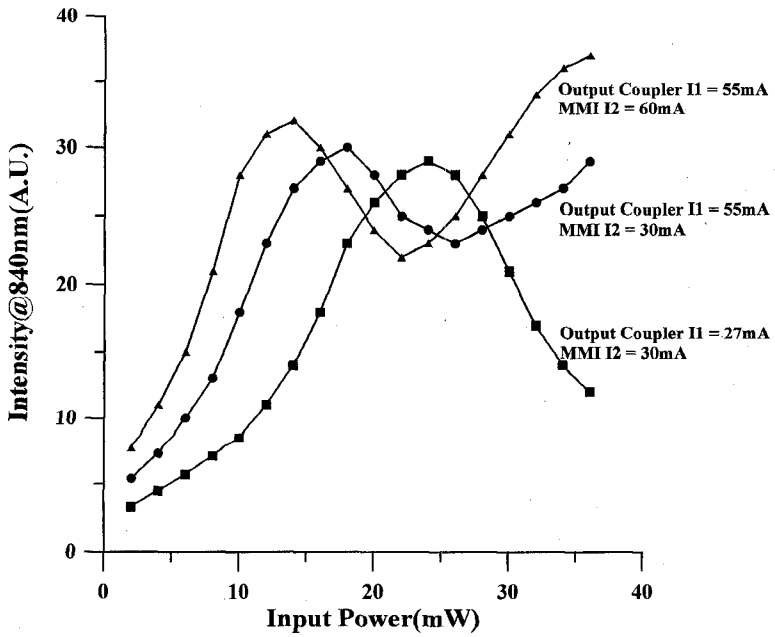

CThO41 Fig. 3. Input-power-dependent switching results with various injection currents.

power variation at the same wavelength. The horizontal axis in Fig. 3 shows the input power before entering the input waveguide. In this measurement, $I_3 = 350$ mA, $I_4 = 221$ mA, and the other two injection currents are shown in the figure. All three curves show depression of output power when the input power reaches certain values. This is a typical power-dependent phenomenon observed in a nonlinear optical-loop mirror. Comparing the data sets of triangles and circles, we can see that different MMI injection currents, which lead to different coupling results, result in different switching threshold values. Meanwhile, a smaller input-output injection current leads to a larger switching threshold. From the data set of squares, we observe a contrast ratio 2.4 between the outputs with inputs at 23 and 35 mW.

CThO42

Ferroelectric-on-silicon modulators for high-density optical interconnects

Feiling Wang, Dean Tsang, Hua Jiang, Kewen K. Li, Vladimir Fuflyigin, *NZ Applied Technologies, 8A Gill Street, Woburn, Massachusetts 01801*

The demonstration of a reflective optical modulator that can be integrated with conventionally processed silicon wafers will be important for dense low-power optical interconnects to silicon complementary metal-oxide semiconductor (CMOS) integrated circuits. Although ferroelectric-film-based optical modulators on silicon substrates were demonstrated,[1] the early work had no active silicon devices. We have successfully fabricated reflection-mode modulators on silicon wafers with active CMOS circuitry using a recently developed low-temperature technique for the growth of ferroelectric films on dielectric mirrors.

The ferroelectric modulator consists of a mirror/ferroelectric/mirror thin film Fabry–Perot structure on a silicon wafer. A lead lanthanum zirconate titanate (PLZT) material[2] with ferroelectric relaxer properties was used as the tunable spacer. The optical length of the ferroelectric layer could be varied by an external electric field through a combination of the electrorefractive and electrostrictive properties of the material. A moderate external field could increase the optical length of the PLZT layer by ~1% and thereby modulate the reflected light.

To prove the feasibility of using ferroelectric modulators for high-density free-space optical interconnects, we fabricated the modulators on silicon wafers with active CMOS circuits and metal-oxide semiconductor field-effect transistor (MOSFET) test structures. Before the fabrication of the modulators, the *I-V* characteristics of the MOSFETs were measured. Reflection-mode modulators of various sizes were then fabricated on the silicon wafers. After completion of the modulators, the characteristics of the MOSFET devices were reexamined, and functionality of the optical modulators was tested. Figure 1 shows a photograph of the silicon wafer with the active MOSFET devices on the left side and the reflection-mode modulators on the right side.

The *I-V* characteristic curves (Fig. 2) taken from a MOSFET device after the modulator fabrication are qualitatively unchanged from the characteristics taken before modulator fabrication. The onset voltage in the *I-V* curves, also observed before the modulator fabrication, was believed to originate from a residual oxide layer in the MOSFET contacts. The functionality of the optical modulators was tested at a wavelength of 633 nm. The intensity modulation of the laser beam reflected from a 500 × 500 μm modulator on the wafer in response to a sinusoidal voltage signal is shown in Fig. 3.

PLZT materials possess inherently fast response speed.[3] Calculations show that 5 ns switching speed is achievable in a 15 × 15 μm modulator using CMOS drivers with 1 mA current. This demonstration of ferroelectric modulators fabricated on conventional CMOS is significant for high-density, low-power parallel optical interconnects to and from silicon-integrated circuits.

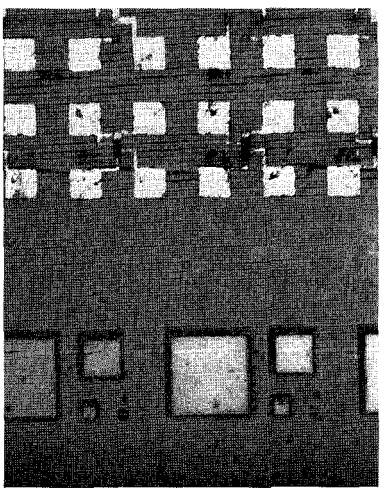

CThO42 Fig. 1. Photograph of a silicon wafer with MOSFET devices on the left side and the ferroelectric thin-film modulators on the right side.

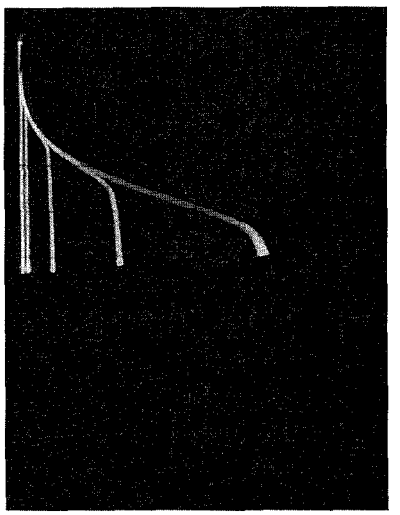

CThO42 Fig. 2. I-V characteristics of a MOSFET after the modulator processing. Vertical scale, 0.1 mA/div.; horizontal scale, 1 V/div.; step generator, 1.0 V/div.

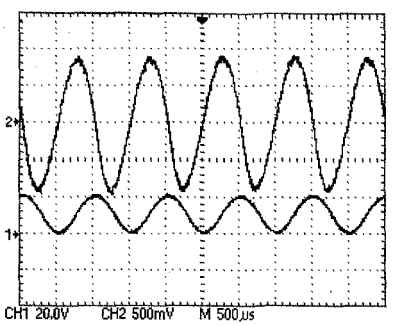

CThO42 Fig. 3. Light-intensity modulation detected from a reflection-mode ferroelectric modulator on a silicon CMOS wafer. Upper trace is the light intensity and lower trace is the applied voltage.

1. F. Wang, G.H. Haertling, Conference on Lasers and Electro-Optics, Vol. 15 of 1995 OSA Technical Digest Series (Optical Society of America, Washington, D.C., 1995).
2. G.H. Haertling, Ferroelectrics **119**, 51 (1991).
3. C. Bao, J.-C. Diels, Conference on Lasers and Electro-Optics, Vol. 15 of 1995 OSA Technical Digest Series (Optical Society of America, Washington, D.C., 1995).

CThO43

Electro-optic effects in asymmetric coupled quantum wells

X. Chen, A. Bhatnagar, M.P. Earnshaw, W. Batty,* D.W.E. Allsopp, *Department of Electronics, University of York, York, England YO1 5DD; E-mail xc2@ohm.york.ac.uk*

Coupled quantum-well systems have been shown from calculations of electroabsorption and subsequent Kramers–Kronig transformation to yield large refractive-index changes with applied electric field.[1–3] Such calculations of refractive-index change in symmetric coupled double quantum wells (QWs) have been shown, by detailed comparison with experiment, to be sensitive to the model used.[4] In this paper, we report a study of the electro-optic properties of a range of asymmetric coupled GaAs-$Al_xGa_{1-x}As$ QW (ACQWs) based on an accurate application of the excitonic Green's-function (EGF) method of Chuang *et al.*[5]

The basic ACQW structure comprises a shallow, wider $Al_xGa_{1-x}As$ well separated from a deep, narrow GaAs well by a barrier that is sufficiently thin (typically ~2 nm) to yield strong coupling between the two wells. The large refractive-index change predicted by Susa[1] and Thirstrup[2] derives principally from a redistribution of oscillator strength between the e1hh1 and e1hh2 transitions as the hh1 (or e1) and hh2 (e2) wave functions localize into QWs of different width and depth when an electric field is applied, while the e1 (h1) wave function remains unchanged.

Figure 1 shows electroabsorption spectra for 60-Å-wide $Al_{0.08}Ga_{0.92}As$ well separated